Cellular Microbiology (2014) **16**(1), 115–130
doi:10.1111/cmi.12184
First published online 12 September 2013

Towards non-invasive monitoring of pathogen–host interactions during *Candida albicans* biofilm formation using *in vivo* bioluminescence

Greetje Vande Velde,[1†] Soňa Kucharíková,[2,3†] Sanne Schrevens,[2,3] Uwe Himmelreich[1‡] and Patrick Van Dijck[2,3*‡]**
[1]*Biomedical MRI/MoSAIC, Department Imaging & Pathology,*
[2]*VIB Department of Molecular Microbiology, and*
[3]*Laboratory of Molecular Cell Biology, KU Leuven, Leuven, Flanders, Belgium.*

Summary

***Candida albicans* is a major human fungal pathogen causing mucosal and deep tissue infections of which the majority is associated with biofilm formation on medical implants. Biofilms have a huge impact on public health, as fungal biofilms are highly resistant against most antimycotics. Animal models of biofilm formation are indispensable for improving our understanding of biofilm development inside the host, their antifungal resistance and their interaction with the host immune defence system. In currently used models, evaluation of biofilm development or the efficacy of antifungal treatment is limited to *ex vivo* analyses, requiring host sacrifice, which excludes longitudinal monitoring of dynamic processes during biofilm formation in the live host. In this study, we have demonstrated for the first time that non-invasive, dynamic imaging and quantification of *in vitro* and *in vivo C. albicans* biofilm formation including morphogenesis from the yeast to hyphae state is feasible by using growth-phase dependent bioluminescent *C. albicans* strains in a subcutaneous catheter model in rodents. We have shown the defect in biofilm formation of a bioluminescent *bcr1* mutant strain. This approach has immediate applications for the screening and validation of antimycotics under *in vivo* conditions, for studying host–biofilm interactions in different transgenic mouse models and for testing the virulence of luminescent *C. albicans* mutants, hereby contributing to a better understanding of the pathogenesis of biofilm-associated yeast infections.**

Introduction

Fungal infections have become increasingly important for environmental, animal and human health (Fisher *et al.*, 2012). In humans, fungal infections caused by yeasts (e.g. *Candida albicans*, *Cryptococcus neoformans*) and molds (e.g. *Aspergillus fumigatus*) have emerged over the past two decades and become more and more significant in clinical practice (Nucci and Marr, 2005; Warnock, 2006; Chen *et al.*, 2010). *C. albicans* is part of the commensal flora of the digestive system and vaginal tract of healthy individuals, but it is also an opportunistic pathogen under certain conditions. *C. albicans* is the most often isolated species in fungal infections (Wisplinghoff *et al.*, 2004; Enoch *et al.*, 2006; Kim and Sudbery, 2011; Pemán and Salavert, 2012). When the host defences are weakened, infections can occur that range from superficial to systemic and even life threatening candidiasis (Wisplinghoff *et al.*, 2004; Kim and Sudbery, 2011). The emergence of fungal diseases is related to an increase in severely ill or immune compromised patients over the past three decades (Eggimann *et al.*, 2003a,b; Nucci and Marr, 2005; Giri and Kindo, 2012). The growing use of implanted medical devices is another reason why the incidence of fungal infections has steadily increased, as many of these infections are emerging from biofilms formed on medical implants (Nucci and Marr, 2005; Pfaller and Diekema, 2010; Giri and Kindo, 2012). They are a major problem in hospitals (Douglas, 2003) as cells in such biofilms are difficult to treat since they are often tolerant to the classical antifungal drugs (Hawser and Douglas, 1995; Lewis *et al.*, 2002). A major challenge in *Candida* biofilm research is the development of suitable models that account for host factors at different infection sites and that allow to evaluate the potential and efficacy of novel antifungal treatment strategies under *in vivo* conditions (Nett and Andes, 2006).

Received 17 July, 2013; revised 12 August, 2013; accepted 14 August, 2013. For correspondence. *E-mail patrick.vandijck@mmbio.vib-kuleuven.be; Tel. (+32) 16 321512; Fax (+32) 16 321979; **E-mail uwe.himmelreich@med.kuleuven.be; Tel. (+32) 16 330925; Fax (+32) 16 330901.
[†]Shared first authors; [‡]Shared last authors.

Among others, an intravenous catheter model (Andes *et al*., 2004) and a subcutaneous catheter model (Řičicová *et al*., 2010) allow *in vivo Candida* biofilm research and have greatly facilitated antifungal testing in small animals (Schinabeck *et al*., 2004; Kucharíková *et al*., 2010; 2013). These models have in common that fungal load in biofilms is analysed *post mortem*, requiring host sacrifice and enumeration of microorganisms from individual biofilms to evaluate the efficacy of antifungal treatment. Also for studying biofilms formed under *in vivo* conditions, evaluation of biofilm properties (architecture, morphology) are limited to *ex vivo* techniques such as microscopic analysis. This approach requires the use of many animals, is labour intensive and only provides one time point per animal and therefore does not enable monitoring of the true time-course of biofilm formation and pathogenesis *in vivo*.

Different imaging modalities are available that enable non-invasive and repeated imaging of targeted cells in living organisms, but especially bioluminescence imaging (BLI) has emerged as a powerful new method to analyse infectious diseases in animal models and microbial viability in particular (Hutchens and Luker, 2007). BLI is based on the detection of visible light (photons) that is produced by an enzymatic oxidation of a substrate, catalysed by luciferase enzymes. It is one of the few imaging methods that can non-invasively quantify cell viability. BLI provides the opportunity to serially and quantitatively monitor infection and microbial load in a single host over time (Sjolinder and Jonsson, 2007). Although BLI is well established for imaging different (microbial) cell populations (Contag *et al*., 1995; Hutchens and Luker, 2007), it is particularly challenging for fungal pathogens (d'Enfert *et al*., 2010; Brock, 2012). Unlike bacteria that can be genetically engineered to express all necessary components for the bioluminescence reaction from the *lux* operon, fungal and other eukaryotic cells depend on external substrate administration for the bioluminescence reaction. Because of their cell wall, the diffusion of the necessary substrate for the light producing reaction is limited, hampering detection of the resulting weak BLI signal *in vivo*, especially from deeper infection sites (Doyle *et al*., 2006). The permeability of hyphal cells to the firefly luciferase substrate luciferin is even more limited resulting in the inability to quantifiable image them during infection (Doyle *et al*., 2006). This was an important obstacle given the importance of the yeast-to-hyphae transition in *C. albicans* virulence (Biswas *et al*., 2007). A *Gaussia princeps* luciferase (*gLuc*) enzyme that is located extracellularly has made BLI of hyphal cells possible, thereby showing substantial improvement in the use of BLI as a tool to monitor superficial *C. albicans* infections (Enjalbert *et al*., 2009). Additionally, yeast and hyphal cell growth could each be visualized *in vitro* by tagging luciferase to cell wall proteins that are specifically expressed in either of these morphological forms (Enjalbert *et al*., 2009). However, the possibility to image the time-course of biofilm formation and morphology transitions during biofilm growth *in vitro* and *in vivo* has not been investigated before. As imaging biofilms in catheters inside the animal poses extra challenges due to light scattering, we explored the feasibility to non-invasively image *C. albicans* biofilm development *in vivo* by using BLI in a subcutaneous catheter model. Furthermore, as the yeast-to-hyphae transition is a key factor involved in *C. albicans* biofilm formation and pathogenicity, we investigated if the time-course of *C. albicans* biofilm morphogenesis under *in vitro* and *in vivo* conditions can be monitored with BLI. We also used BLI to monitor the effect on biofilm formation of the *C. albicans* Bcr1 gene which plays a central role in *in vitro* and *in vivo* substrate adhesion and biofilm formation, by using a bioluminescent *BCR1* deletion strain.

Results

Minimizing background signal for BLI

Catheters are often made radio-opaque to enable the assessment of the catheter position inside the body. For example, barium sulfate filler is added to make the catheter visible under fluoroscopy and on X-ray images. However, barium sulfate phosphoresces. Therefore, we tested different intravenous catheters for background luminescence when imaged with BLI and found two out of three to be highly phosphorescent *in vitro* (Fig. 1 panel A and Fig. S1), which is a confounding factor for evaluating the specific bioluminescent signal and signal kinetics from *gLuc*-expressing *C. albicans* biofilms *in vitro*.

To assess the relevance of this phosphorescence background signal from the catheters for BLI *in vivo*, catheters containing biofilms of *ACTgLuc*-expressing *C. albicans* and empty catheter pieces were implanted subcutaneously. After catheter implantation and after 2 and 6 days of biofilm maturation, the mice were imaged by BLI. Images acquired sequentially before and after opening the scanner door and with or without addition of coelenterazine (CTZ) – the substrate used for the bioluminescence reaction – were compared. At all time points, we detected a clearly visible signal from empty implanted Arrow catheters without addition of CTZ (Fig. 1 panels B and C). This signal increased significantly every time the animals were exposed to light (i.e. when opening the scanner door), indicating that the detected signal originated from phosphorescence of the catheter pieces. Next, we opened the door and added CTZ to the catheters and compared the specific BLI signal from biofilms of *ACTgLuc*-expressing cells with light emanating from empty catheters. Unlike for the empty catheters, the BLI

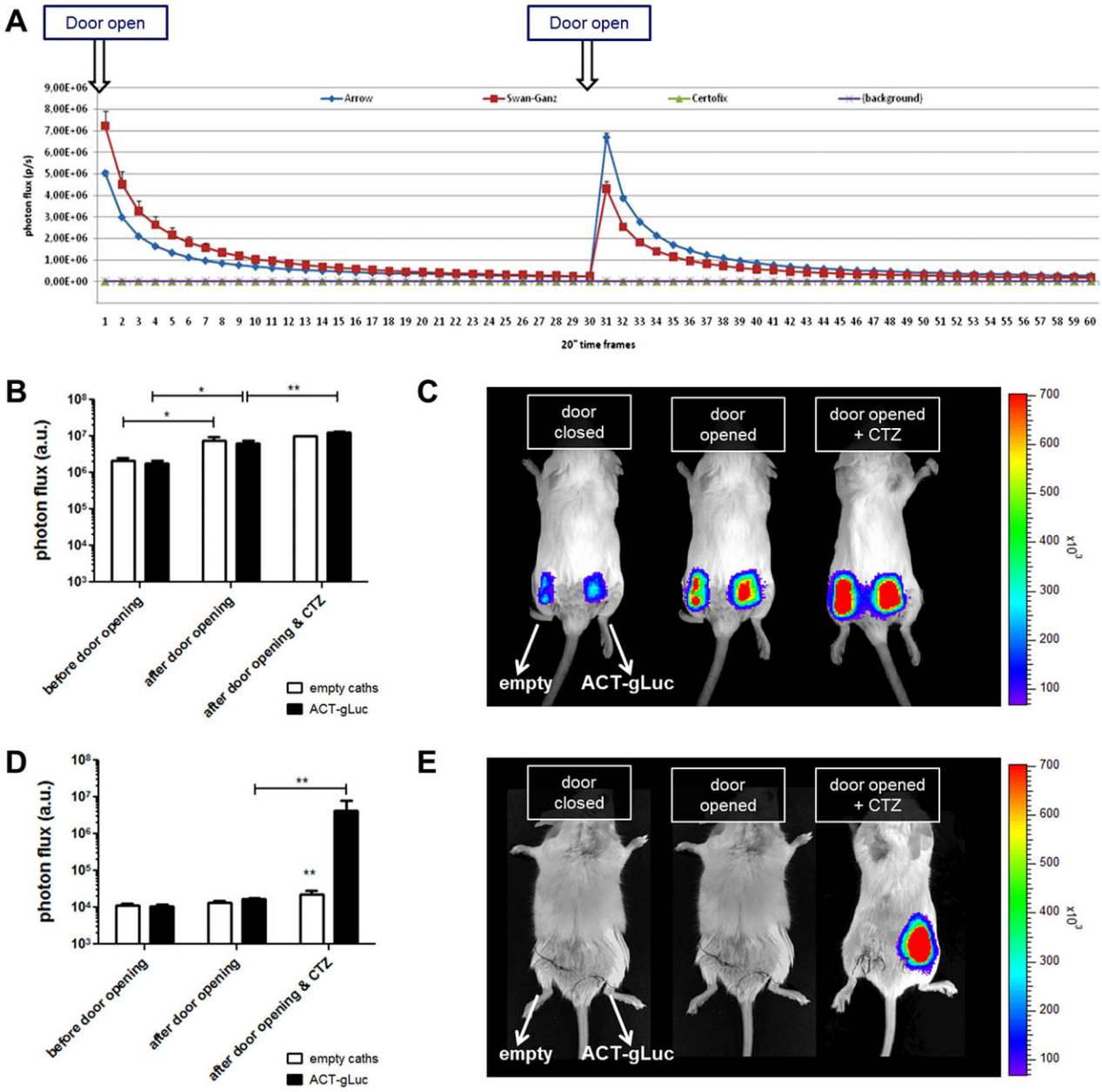

Fig. 1. Phosphorescence of different common catheter types.
A. Three different brands of triple lumen catheters (Arrow, Edwards Swan-Ganz, BBraun Certofix) were cut in 1 cm long pieces and 60 consecutive 20 s-frames were acquired with the BLI camera and compared with the background signal (see Fig. S1). Before the sequence and after the 30th imaging frame, the catheters were exposed to light by opening-closing of the scanner door (arrows). Edwards Swan-Ganz and Arrow catheter fragments clearly showed phosphorescence signal after exposure to daylight, decaying over time. For the BBraun Certofix catheter, no phosphorescence was detected and its signal intensity was equal to background.
B and D. Quantification of the *in vivo* luminescence signal from empty catheter pieces and catheter pieces carrying biofilms formed by SKCA23-*ACTgLuc C. albicans* cells, acquired at 2 days after catheter implantation, using Arrow (B) and Certofix (E) catheters.
C and E. *In vivo* BLI images from a representative mouse at the 2 days' time point are shown, acquired after keeping the scanner door closed, after opening of the scanner door and after opening of the scanner door and CTZ administration, using Arrow (C) and Certofix (E) catheters (Error bars represent SD of triplicate samples; $*P < 0.05$, $**P < 0.005$, $***P < 0.0005$).

signal intensity from catheters containing *ACTgLuc*-expressing cells increased significantly above the phosphorescence signal upon CTZ addition (Fig. 1 panels B and C). However, the additional increase in luminescence upon CTZ addition was relatively small compared with the increase in catheter phosphorescence upon opening of the scanner door. Performing the same *in vivo* experiment using non-phosphorescent catheters (Certofix),

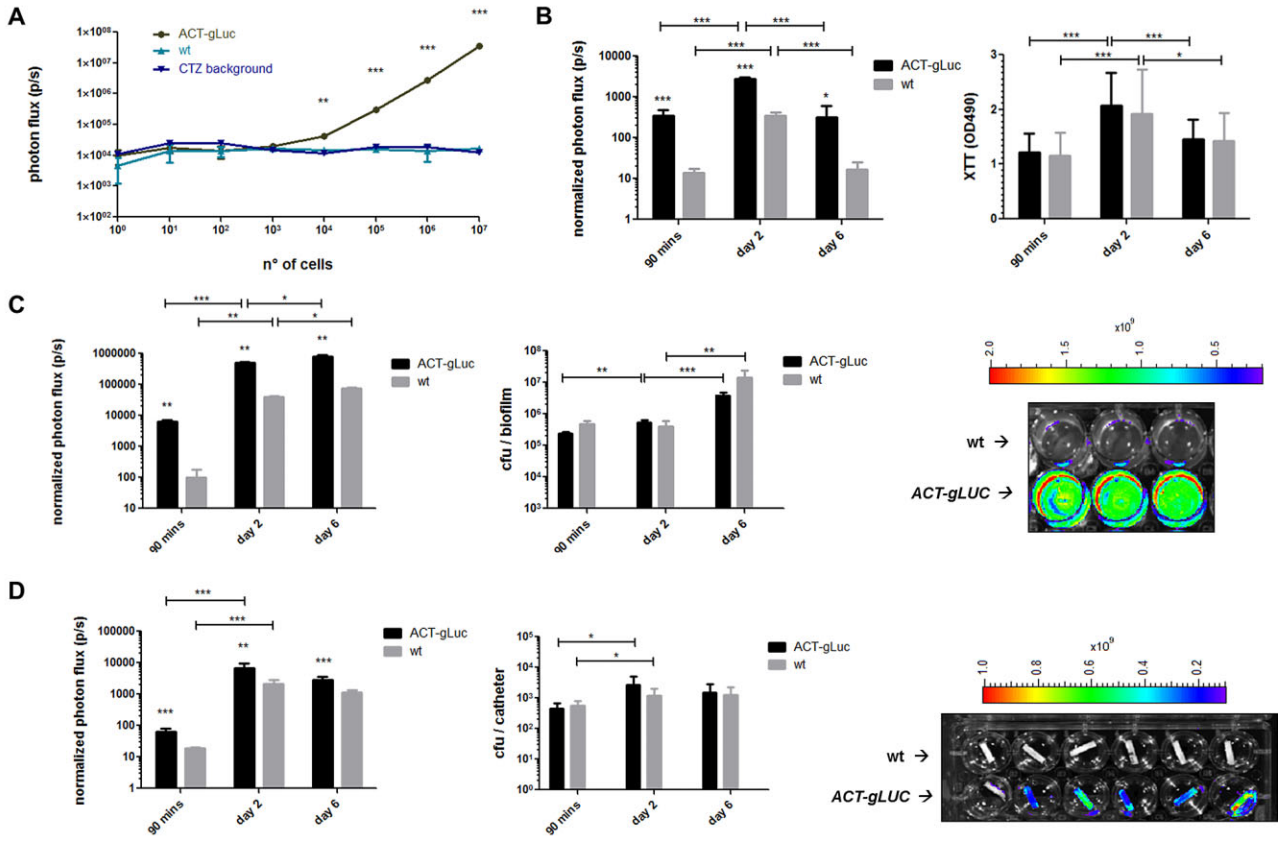

Fig. 2. BLI of *in vitro C. albicans* biofilm formation.
A. BLI of 10-fold dilutions of SKCA23-*ACTgLuc* and SC5314 (wt control) *C. albicans* cells, and CTZ alone ($n = 3$). *In vitro* detectability was established to be $\geq 10^4$ cells.
B. BLI signal intensity and metabolic activity measurements of biofilms formed by SKCA23-*ACTgLuc* and SC5314 *C. albicans* cells on the bottom of 96-well plates ($n = 6$).
C. BLI signal and cfu quantification of biofilms formed by SKCA23-*ACTgLuc* and SC5314 *C. albicans* cells on the bottom of 24-well plates ($n = 3$). A typical BLI image of 2-day-old mature biofilms is shown on the right ($n = 3$ per strain).
D. Graphs of BLI signal intensity and cfu quantification of biofilms formed by SKCA23-*ACTgLuc* and SC5314 *C. albicans* cells in catheter pieces ($n = 6$). A typical BLI image of 2-day-old mature biofilms formed on the inside of catheter pieces ($n = 6$ per strain) is shown on the right (Error bars indicate SD of replicate samples; $^*P < 0.05$, $^{**}P < 0.005$, $^{***}P < 0.0005$).

no phosphorescent background signal could be detected after exposing the animals to light (Fig. 1 panel E). A significant BLI signal above background could clearly be visualized and quantified only upon addition of CTZ to catheters containing biofilms formed by *ACTgLuc*-expressing *Candida* cells (Fig. 1 panels D and E). Therefore, and to avoid complications in signal analysis due to different kinetics of the phosphorescence and *ACTgLuc*-induced BLI signals, we have used non-phosphorescent catheters (Certofix) for all further *in vitro* and *in vivo* BLI experiments. Biofilms formed on the non-phosphorescent catheters showed the same properties regarding biofilm formation (data not shown) and were therefore comparable to biofilms formed on the catheters used in previous studies (Kucharíková *et al.*, 2010; Řičicová *et al.*, 2010).

BLI of in vitro *biofilm formation*

CTZ is known to undergo some auto-oxidation in the presence of oxygen, contributing to a background BLI signal (Shimomura *et al.*, 1993; Tannous *et al.*, 2005). Therefore, we determined the minimum number of *ACTgLuc*-expressing *C. albicans* cells in suspension that resulted in a detectable BLI signal, significantly above the background signal. A fixed CTZ concentration was added to empty wells and to 10-fold dilution series of *ACTgLuc*-expressing and wild-type (wt) *C. albicans* cells (Fig. 2, panel A). The BLI signal intensity measured from 10^4 or more *ACTgLuc*-expressing *C. albicans* cells was found to be significantly higher than the background signal originating from auto-oxidation of CTZ alone or incubated with non-luminescent wt cells. The specific BLI signal strongly

correlated with the amount of *ACTgLuc*-expressing *C. albicans* cells ($R^2 = 0.998$).

To investigate the feasibility of using BLI for imaging biofilm development, we first evaluated the BLI signal intensity from *C. albicans* biofilms formed on the bottom of polystyrene cell culture plates *in vitro*. *ACTgLuc*-expressing and wt *C. albicans* cells were allowed to adhere to the bottom of 96- and 24-well cell culture plates and incubated for mature biofilms to be formed. BLI was performed after 90 min (period of adhesion) and after 2 and 6 days of mature biofilm formation. At every imaging time point, the metabolic activity of the biofilm forming cells (in 96-well plates) and colony-forming units (cfu) (in 24-well plates) were quantified. At all imaging time points, the BLI signal from *ACTgLuc*-expressing biofilms formed on 96-well plates was significantly higher than from wt biofilms (Fig. 2, panel B). Two days after adhesion, the BLI signal was significantly increased for *ACTgLuc*-expressing biofilms, which is consistent with mature biofilm development at this stage (Kucharíková *et al*., 2011). The noticeable finding that the BLI signal from wt biofilms was also increased can probably be attributed to the increase of organic matter in the extracellular matrix, which might stimulate CTZ auto-oxidation. The BLI signal of 6-day-old biofilms was decreased, which can be explained by a limitation in nutrients, which corresponds to the metabolic activity of the cells in the biofilm measured by the XTT (2,3-Bis-(2-Methoxy-4-Nitro-5-Sulfophenyl)-2H-Tetrazolium-5-Carboxanilide) assay. Overall, the BLI data was in agreement with the metabolic activity of the biofilm forming cells as measured by the XTT reduction assay (Fig. 2, panel B).

For biofilms formed in 24-well plates, nutrients are less likely to be a limiting factor for biofilm development compared with biofilms formed in 96-well plates. Indeed, the BLI signal intensity from biofilms formed by *ACTgLuc*-expressing *C. albicans* as well as from wt cells increased significantly after 2 and 6 days of mature biofilm formation, which was corroborated by a significant increase of cfu over time (Fig. 2, panel C). Importantly, the BLI signal from *ACTgLuc*-expressing *C. albicans* biofilms was at every imaging time point significantly higher than the background BLI signal measured from wt *C. albicans* biofilms, for the same amount of cfu per biofilm (Fig. 2, panel C).

We next evaluated the BLI signal intensity from biofilms formed inside polyurethane catheter pieces *in vitro*. Similar to the results for biofilms formed on cell culture plates, the specific BLI signal from *ACTgLuc*-expressing biofilms was at every imaging time point significantly higher than the background BLI signal measured from wt biofilms. From the period of adhesion (90 min) towards mature biofilm formation on day 2, the BLI signal increased significantly for both *ACTgLuc*-expressing and wt biofilms (Fig. 2, panel D). From day 2 to day 6 of biofilm maturation, the BLI signal intensity remained at the same level. These BLI results were in agreement with the cfu retrieved from each biofilm that were also significantly increased on day 2 and remained unchanged by day 6 (Fig. 2, panel D).

Taken together, our data indicate that BLI can be used as a sensitive tool to monitor *in vitro* biofilm development on foreign bodies, including on biofilms formed on the inside of catheter pieces.

BLI of biofilms formed in vivo

We evaluated the feasibility to non-invasively follow-up *in vivo* biofilm development in subcutaneously implanted catheters with BLI. Hereto, three catheters inoculated with wt *C. albicans* cells were implanted on the left side and three catheters inoculated with *ACTgLuc*-expressing *C. albicans* were implanted on the right side under the skin of the lower back of mice ($n = 12$). *In vivo* biofilm formation was visualized with repeated BLI starting on the same day of catheter implantation, and after 2 and 6 days of mature biofilm formation. Catheter pieces ($n = 4$ per *C. albicans* strain) were handled in parallel with the catheters for implantation, imaged *in vitro* with BLI and used for quantification of cfu at the adhesion time point to verify adhesion of equal numbers of cells on all catheters at the time of implantation. After catheter implantation ($n = 12$) and after 2 days ($n = 12$), all mice were imaged with BLI. After the 2 days' imaging time point, half of them ($n = 6$) were sacrificed for catheter explantation and *ex vivo* quantification of biomass for validation of the BLI results. At the 6 days' imaging time point, the remaining half of the group ($n = 6$) was imaged and sacrificed thereafter for catheter explantation.

At every imaging time point, a significant BLI signal above background was detected from *ACTgLuc*-expressing biofilms formed on the inside of catheters *in vivo*, while *ACTgLuc*-expressing and wt biofilms were verified to contain the same amount of cfu per biofilm (Fig. 3, panel A). The BLI signal could clearly be visualized and followed up over time in every individual animal (Fig. 3, panel B) and was in agreement with the amount of cfu quantified from the biofilms (Fig. 3, panel A). Interestingly, wt biofilms elicited a significant BLI signal above background at all time points, as was also observed for the *in vitro* biofilm BLI experiments (Fig. 2). However, at every imaging time point, the BLI signal quantified from *ACTgLuc*-expressing biofilms was at least one order of magnitude (i.e. log10) and significantly higher than the background signal of wt biofilms, indicating that BLI can be used for longitudinal monitoring and quantification of *in vivo* biofilm development on implanted catheters.

As bioluminescence images represent low-resolution 2D projections overlaid on a planar photographic image,

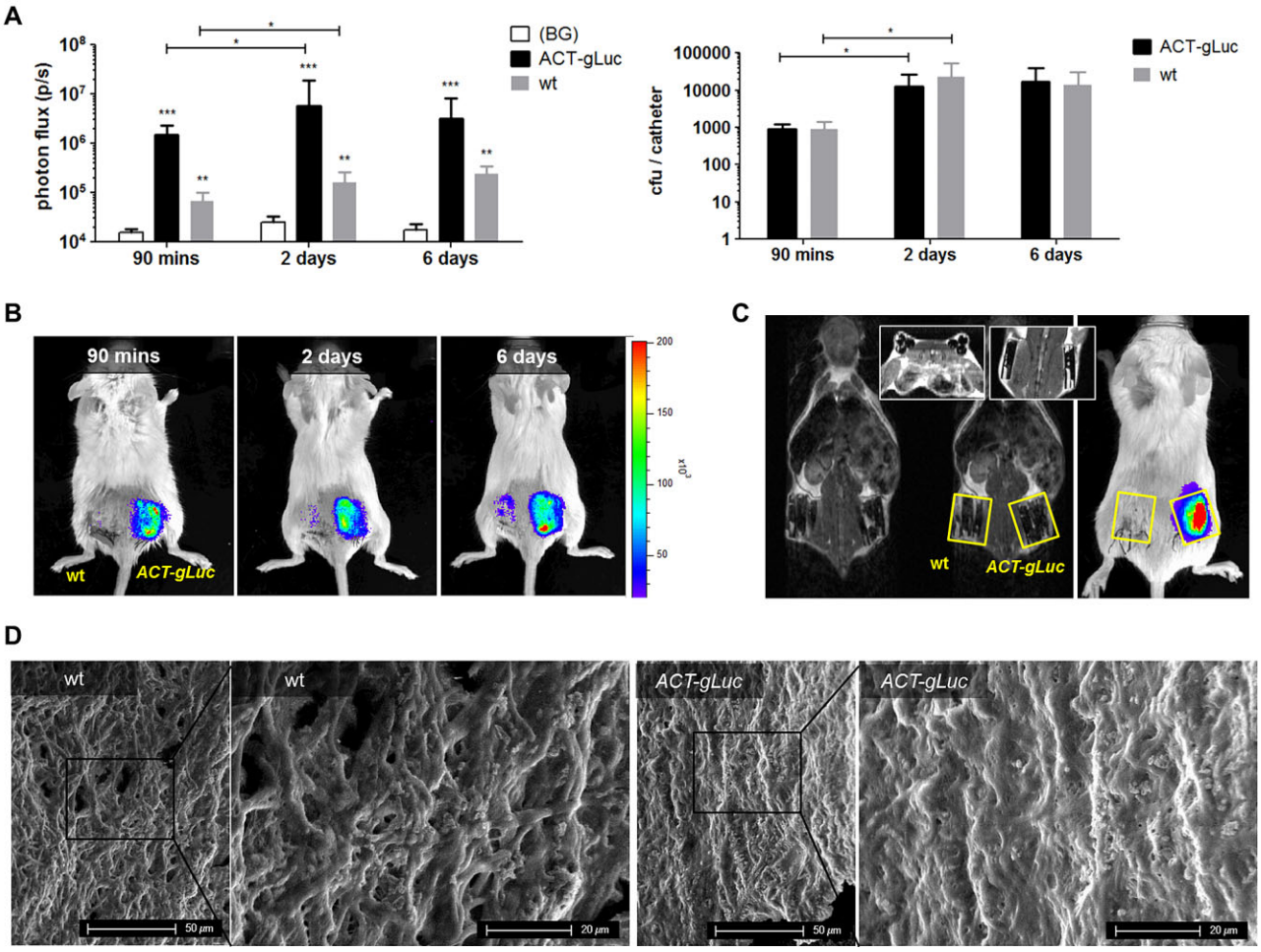

Fig. 3. BLI of *in vivo* biofilm formation.
A. *In vivo* BLI signal quantification from biofilms formed by SKCA23-*ACTgLuc* and SC5314 (wt) *C. albicans* cells on implanted catheter pieces, after catheter implantation (90 min, $n = 12$ mice) and after 2 ($n = 12$ mice) and 6 days ($n = 6$ mice) of *in vivo* biofilm development, compared with the background (BG) BLI signal from a subcutaneous CTZ injection. The graphs on the right represent cfu quantified from biofilms formed by SKCA23-*ACTgLuc* and SC5314 *C. albicans* cells at the time of implantation (90 min, $n = 4$ per strain) or explanted from mice after 2 and 6 days ($n = 18$ per strain) (Error bars indicate SD of replicate samples; $^{*}P < 0.05$, $^{**}P < 0.005$, $^{***}P < 0.0005$).
B. *In vivo* BLI images from one representative (i.e. showing average BLI signal) mouse imaged at three different time points after catheter implantation are shown.
C. in parallel with BLI, MR images were acquired to visualize the exact three-dimensional catheter position for verifying correct ROI placement and quantification of the BLI signal. Two adjacent slices from a typical MRI dataset overlaid with ROIs for photon flux quantification (yellow rectangles) are shown on the left with the corresponding BLI image on the right.
D. SEM of 6-day-old mature biofilms formed by *C. albicans* SC5314 (wt, on the left) and SKCA23-*ACTgLuc* (on the right) inside polyurethane catheter fragments *in vivo*. After explantation, the catheters were longitudinally cut and fixed before SEM. Magnification of the left panels is 500× (scale bars measure 50 μm). The right panels are 1200× magnifications of the black boxed area (scale bars measure 20 μm).

individual catheters might not always be clearly visible on the resulting image. Therefore, signal quantification may potentially suffer from variability due to implantation depth and/or incorrect delineation of the catheters. Also, light absorption due to scar formation or unexpected bleedings may affect BLI quantification. We have therefore acquired high-resolution magnetic resonance (MR) images while the animals were still anesthetized from BLI and fixed to the same reference frame, i.e. animal holder. Anatomical details and the position of the catheters as visualized on the MR images were used for delineation of the region of interests (ROIs) used for subsequent BLI signal quantification (Fig. 3, panel C). In order to explore the potential of MRI to improve the accuracy of BLI signal quantification, the BLI signal quantified from correctly positioned ROIs using prior knowledge from the MR images was compared with BLI signal intensities quantified from ROIs that were placed over the focus of the BLI signal spot while varying the angulation of the ROI. No significant influence from different angulations of the ROIs could be found (data not

shown), which indicates that fine-tuning of the ROI position is not a prerequisite for accurate BLI quantification in animal models of subcutaneously implanted catheters. For all animals, we confirmed a similar implantation depth of the catheters and the absence of bleedings or the formation of major scar tissue between the catheters and the skin of the animals.

To investigate a possible unwanted effect of *ACTgLuc*-transgene expression on the biofilm structure, catheters carrying biofilms maturing under *in vivo* conditions explanted at 6 days after implantation were examined by scanning electron microscopy (SEM) as described before (Řičicová *et al*., 2010). It was verified that *ACTgLuc*-transgene expression did not alter the *in vivo* biofilm architecture (Fig. 3, panel D).

BLI of C. albicans *morphogenesis during biofilm development*

In a next step, we investigated whether the expression of *gLuc* under control of a morphogenesis-dependent promoter can be applied for BLI of the *C. albicans* yeast-to-hyphae transition during biofilm formation. For these experiments, we used the CEC971-*HWPgLuc C. albicans* strain (Enjalbert *et al*., 2009), which expresses *gLuc* under control of a hyphal promoter that becomes active when cells undergo yeast-to-hyphae transition (Staab *et al*., 1996). As a control, we used a strain that expresses *gLuc* under control of the constitutively active *ACT1* promoter, i.e. in both the yeast and hyphal forms (CEC988-*ACTgLuc*).

First, we determined the BLI signal of 10-fold dilution series of CEC988-*ACTgLuc*, CEC971-*HWPgLuc*, DAY185 (wt control) *C. albicans* cell suspensions and CTZ alone. The BLI signal intensity from the cells expressing *gLuc* under control of the *HWP1* promoter was equal to the background BLI signal from the controls. A specific BLI signal that correlated with the number of cells could only be detected for *C. albicans* expressing *gLuc* under control of the *ACT1* promoter ($R^2 = 0.998$, Fig. 4, panel A). These results are in line with *C. albicans* cells known to be in the yeast form in serum-free medium (Sudbery, 2011). Next, we tested whether the transition from the yeast form to the hyphal form can be monitored with BLI, which is known to be stimulated by adding serum to the medium (Sudbery, 2011). We incubated wt, *ACTgLuc*- and *HWPgLuc*-expressing cells with and without fetal bovine serum (FBS) (10%) in the culture medium and imaged them after 1.5 h and 4.5 h with BLI. The relative increase in BLI signal intensity from *HWPgLuc*-expressing cells grown in medium compared with serum-free medium was significantly higher than the increase in signal intensity measured from wt and *ACTgLuc*-expressing cells, both after 1.5 h and 4.5 h of incubation (Fig. 4, panel B). These results demonstrate that BLI can be used to quantify hyphal growth *in vitro*.

Furthermore, we evaluated whether the hyphal growth during *in vitro* biofilm formation in catheter pieces can be followed with BLI. Catheters were incubated with *ACTgLuc*- ($n = 12$) or *HWPgLuc*-expressing *C. albicans* ($n = 12$) in medium containing FBS, which is known to stimulate yeast-to-hyphae transition (Sudbery, 2011). After 90 min, 2 days, 6 days and 9 days of biofilm growth, three catheters of each strain were imaged with BLI, followed by cfu quantification. At each time point, the number of cfu recovered from biofilms formed by each strain was equal, confirming that differences in BLI signal intensity between the strains were not due to differences in the amount of biofilm forming cells (Fig. 4, panel C). After 90 min of *C. albicans* cell adhesion on the catheters, a significantly lower BLI signal intensity was detected from *HWPgLuc*-expressing *C. albicans* cells compared with *ACTgLuc*-expressing cells, corresponding to the lower numbers of *C. albicans* hyphal cells compared with yeast cells, characteristic at this stage (Blankenship and Mitchell, 2006). After 2 days of biofilm growth, the BLI signal intensities from both yeast as well as hyphal cells showed to be significantly increased due to biofilm proliferation, whereas after 6 days they remained at the same levels when the mature biofilm is maintained. That *HWPgLuc*-expressing *C. albicans* cells showed a more pronounced BLI signal intensity increase during the first days of biofilm formation relative to *ACTgLuc*-expressing cells corresponds to hyphal growth in addition to cell proliferation during mature biofilm development. After 9 days of *in vitro* biofilm growth, the BLI signal intensity from both *ACTgLuc*- and *HWPgLuc*-expressing biofilms has decreased, which is in agreement with the lower cell numbers (cfu) recovered from the catheters.

In order to demonstrate the potential of BLI to non-destructively determine the yeast-to-hyphal cell ratio, we imaged *HWPgLuc*-expressing *C. albicans* cells that were either in the yeast or hyphal stage, or as mixtures at different ratios of yeast to hyphal cells. The percentage of yeast to hyphal cells could be calculated from the bioluminescence signal of the samples (Fig. S2), demonstrating that the yeast-to-hyphae ratio can be determined by using BLI.

To verify whether BLI can be used as a technique to non-invasively follow up on hyphal growth *in vivo*, catheters inoculated with *ACTgLuc*- or *HWPgLuc*-expressing *C. albicans* were implanted on the back of mice ($n = 6$). All mice were repeatedly monitored with BLI on the same day of catheter implantation (adhesion of *C. albicans* cells to the catheters) and after 2, 6 and 9 days of biofilm maturation. After catheter implantation, all mice exhibited a significantly lower BLI signal intensity

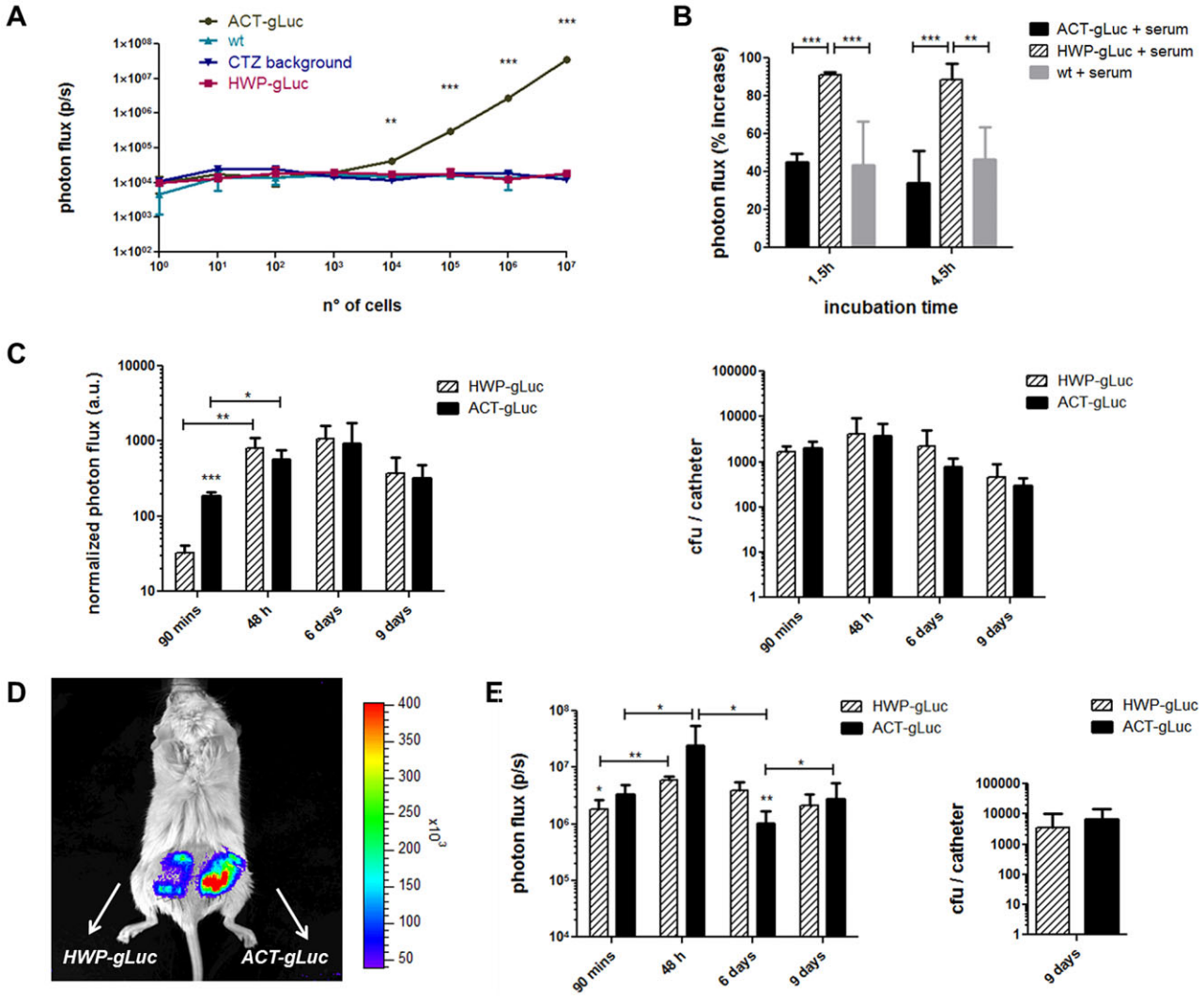

Fig. 4. *In vitro* and *in vivo* BLI of *C. albicans* morphogenesis during *in vitro* and *in vivo* biofilm formation.
A. *In vitro* BLI of 10-fold dilutions of CEC988-*ACTgLuc*, CEC971-*HWPgLuc*, DAY185 (wt control) *C. albicans* cell suspensions in serum-free medium and CTZ alone.
B. *In vitro* BLI of the yeast-to hyphae transition of CEC988-*ACTgLuc*, CEC971-*HWPgLuc*, DAY185 (wt control) *C. albicans* cell suspensions upon incubation for 1.5 h and 4.5 h in serum-containing medium compared with serum-free medium. The data is represented as the relative increase in BLI signal upon incubation in serum-containing medium relative to the BLI signal from cell suspensions incubated in serum-free medium ($n = 3$ per condition and strain).
C. *in vitro* BLI signal and cfu quantification from biofilms formed by CEC988-*ACTgLuc* and CEC971-*HWPgLuc C. albicans* cells on catheter pieces ($n = 3$).
D. Representative *in vivo* BLI image of an average mouse at the same day after catheter implantation.
E. *In vivo* BLI signal ($n = 6$ mice) and cfu ($n = 18$ catheters) quantified from biofilms formed by CEC988-*ACTgLuc* and CEC971-*HWPgLuc C. albicans* in implanted catheter pieces (Error bars indicate SD of replicate samples; $^{*}P < 0.05$, $^{**}P < 0.005$, $^{***}P < 0.0005$).

from *HWPgLuc*-inoculated catheters (Fig. 4, panel D and E). After two days of biofilm maturation, there was a more pronounced and significant increase in the BLI signal for *HWPgLuc*-expressing *C. albicans* biofilms compared with *ACTgLuc*-expressing biofilms, indicating hyphal growth. When the biofilm matures further, the BLI signal from *ACTgLuc*-expressing biofilms showed a decrease whereas the BLI signal from *HWPgLuc*-expressing biofilms remained largely unchanged. This may point to the mainly hyphal content of biofilms of this age (Nett and Andes, 2006). After the last imaging time point at day nine, the mice ($n = 6$) were sacrificed and cfu were quantified from explanted catheters, confirming that biomass was comparable among all biofilms (Fig. 4, panel E). Taken together, the data indicate that BLI can be used to monitor hyphal growth during *in vitro* and *in vivo* biofilm formation, which is most pronounced during the earliest stage of biofilm development.

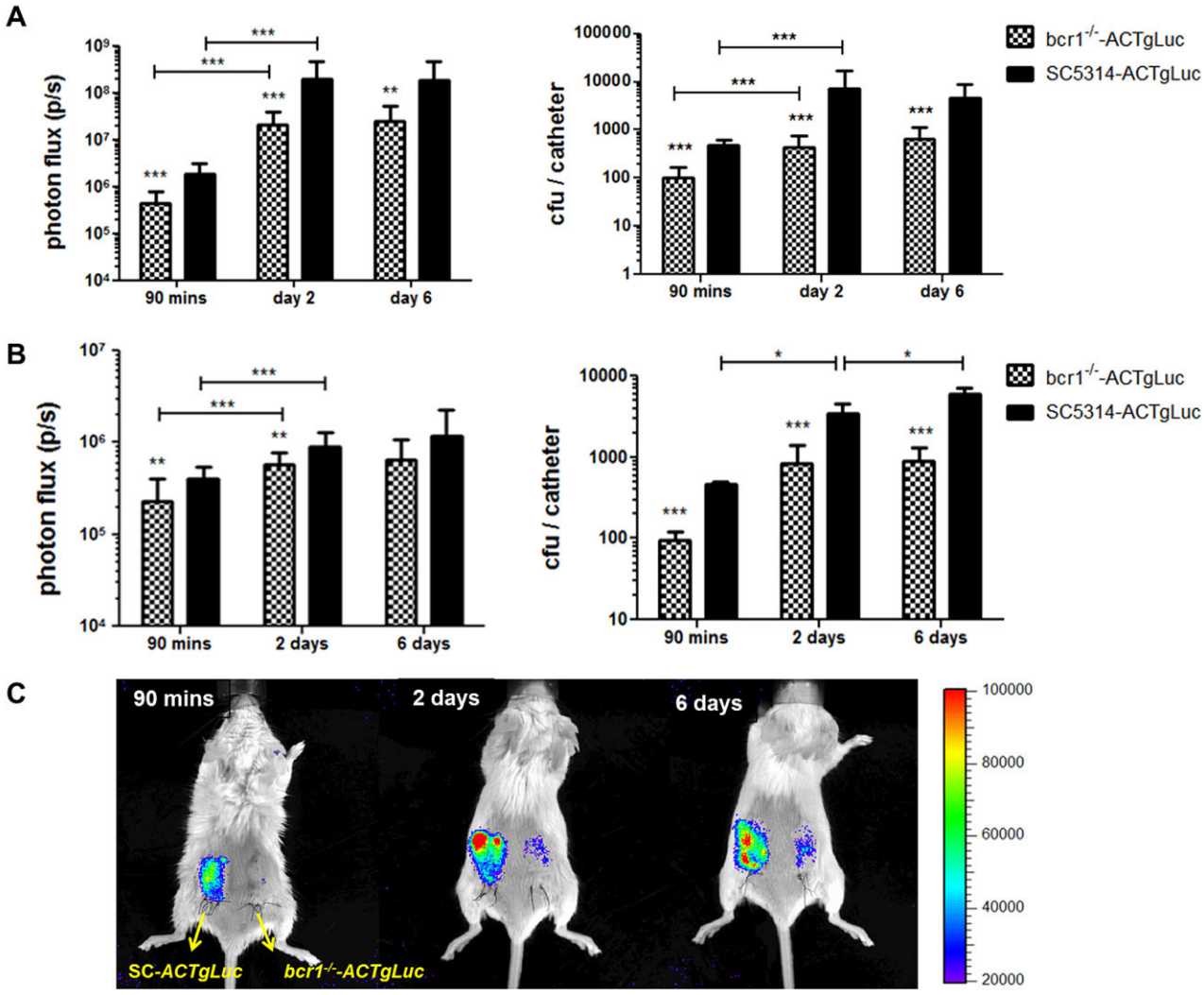

Fig. 5. *In vitro* and *in vivo* BLI of defective adhesion and biofilm formation.
A. Graphs of BLI signal intensity and cfu quantification of (defective) biofilm formation by *bcr1*$^{-/-}$*-ACTgLuc* and SC-*ACTgLuc C. albicans* cells in catheter pieces ($n = 6$).
B. *In vivo* BLI signal quantification (left graph) from biofilms formed by *bcr1*$^{-/-}$*-ACTgLuc* and SC-*ACTgLuc C. albicans* cells on implanted catheter pieces, after catheter implantation (90 min, $n = 12$ mice) and after 2 ($n = 12$ mice) and 6 days ($n = 6$ mice) of *in vivo* biofilm development. The graph on the right represents cfu quantified from biofilms formed by *bcr1*$^{-/-}$*-ACTgLuc* and SC-*ACTgLuc C. albicans* cells at the time of implantation (90 min, $n = 4$ per strain) or explanted from mice after 2 and 6 days ($n = 18$ per strain).
C. *In vivo* BLI images from one representative (i.e. showing average BLI signal) mouse imaged at three different time points after catheter implantation are shown (Error bars indicate SD of replicate samples; *$P < 0.05$, **$P < 0.005$, ***$P < 0.0005$).

BLI of defective biofilm formation by BCR1 mutant C. albicans

In the next series of experiments, we aimed to use and validate BLI to identify biofilm-defective mutants. For these experiments, we used a *C. albicans BCR1* knockout strain that was engineered to constitutively express *gLuc* on its cell wall in order to non-invasively image its capacity to adhere to and form biofilms inside catheters. The bioluminescence emitted by this *ACTgLuc*-expressing *bcr1*$^{-/-}$ strain showed to be directly comparable to the bioluminescence of the *ACTgLuc*-expressing strain (SKCA23-*ACTgLuc*), used as wild type control for biofilm formation in the following experiments (Fig. S3, panel A).

First, we used BLI to evaluate the capacity of *ACTgLuc*-expressing *bcr1*$^{-/-}$ *C. albicans* cells to adhere and to form biofilms on catheter pieces *in vitro*. After *C. albicans* adhesion on the catheters, a significantly lower BLI signal was detected from catheters inoculated with *bcr1*$^{-/-}$*-ACTgLuc* compared with those inoculated with SC-*ACTgLuc* (Fig. 5, panel A). This corresponds to the lower numbers

of *bcr1*$^{-/-}$ *Candida* cells compared with wt that were able to attach onto the catheter, which is in agreement with the known adhesion defect of this strain (Nobile *et al*., 2006; Řičicová *et al*., 2010). After 2 days and 6 days of mature biofilm formation, significantly lower BLI signal intensities were detected from catheter pieces inoculated with *bcr1*$^{-/-}$*-ACTgLuc* compared with the SC-*ACTgLuc* strain (Fig. 5, panel A), indicating the inability of the *bcr1* mutant strain to form normal biofilms. The lower BLI signal intensities emanating from *bcr1*$^{-/-}$*-ACTgLuc*-inoculated catheters corresponded to significantly reduced numbers of cfu recovered from these catheters compared with the control strain, validating BLI as a technique to monitor defective adhesion and biofilm formation of the *bcr1*$^{-/-}$ *C. albicans* strain on catheters under *in vitro* conditions.

To evaluate the biofilm forming capability of *bcr1*$^{-/-}$ mutant *C. albicans* under *in vivo* conditions with BLI, catheters inoculated with *ACTgLuc*-expressing *bcr1*$^{-/-}$ and wt strains were implanted on the back of mice ($n = 12$). All mice were imaged with BLI after catheter implantation ($n = 12$) and after 2 days ($n = 12$). After the 2 days' imaging time point, half of the mice ($n = 6$) were sacrificed for catheter explantation and *ex vivo* quantification of cfu. At the 6 days' imaging time point, the remaining half of the group ($n = 6$) was imaged and sacrificed thereafter for catheter explantation and validation of the imaging results. Catheter pieces ($n = 4$ per strain) were handled in parallel with the catheters for implantation and used for quantification of cfu, to evaluate the adhesion properties of the *Candida* strain at the time of implantation. *In vivo* BLI revealed significantly lower BLI signal intensities for the *bcr1*$^{-/-}$*-ACTgLuc*-inoculated catheters compared with SC-*ACTgLuc*-inoculated catheters, illustrating the hampered adhesion properties of this strain. This was confirmed by the cfu retrieved from the catheters at the time of implantation (Fig. 5, panels B and C). Also at the following *in vivo* imaging time points (2 and 6 days), the BLI signal intensity from *bcr1*$^{-/-}$*-ACTgLuc*-inoculated catheters was significantly lower than the signal from *ACTgLuc*-expressing control biofilms, demonstrating the inability of the *bcr1*$^{-/-}$-strain to form normal biofilms under *in vivo* conditions (Fig. 5, panels B and C). This was clearly visualized for every individual animal (Fig. 5, panel C). The imaging results were at all time points in agreement with the amount of cfu quantified from the biofilms (Fig. 5, panel B) and defective *in vitro* and *in vivo* biofilm formation by the *bcr1*$^{-/-}$*-ACTgLuc*-strain was confirmed by SEM (data not shown) as shown before (Řičicová *et al*., 2010).

In the context of assessing adherence properties and biofilm forming capabilities of a mutant *Candida* strain that is potentially defective for biofilm formation, it becomes relevant to evaluate the bioluminescence emitted by biofilm cells versus planktonic cells that are not associated with a biofilm structure. In order to evaluate to what extent planktonic cells that are not attached to mature biofilm structures contribute to the overall *in vivo* BLI signal, we collected the free floating cells from inside the lumen of the explanted catheters and compared them with the biofilm that remains adhered to the catheters. Comparing the BLI signal of the cells in the washing fluid with the overall *in vivo* BLI signal emanating from biofilms formed on implanted catheters (compare Fig. S3, panel B with Fig. 5, panel B), the BLI signal intensity is at least one order of magnitude lower, showing that the BLI signal of planktonic cells not associated with the biofilm structure form only a minor fraction and have only a marginal contribution to the overall *in vivo* BLI signal. Interestingly, after 2 days of biofilm formation, a significantly lower BLI signal intensity, close to background, was measured for *bcr1*$^{-/-}$*-ACTgLuc*-inoculated catheters, due to a large fraction of catheters for which zero cfu of planktonic cells were recovered from the catheter lumen (89% for *bcr1*$^{-/-}$*-ACTgLuc*-inoculated catheters versus 39% for *ACTgLuc*-expressing control biofilms). This illustrates that the overall *in vivo* BLI signal reflects the biomass associated with the catheter, with a negligible contribution from loose planktonic cells in the catheter lumen. Quantification of the cfu corroborated the BLI results for the washing fluid, confirming that BLI is a valid technique to conveniently assess planktonic versus biofilm-associated cells on subcutaneously implanted catheters *in vivo*.

Taken together, our data illustrate that BLI is a powerful technique to monitor and quantify the adhesion between *C. albicans* strains and the substrate, as well as further biofilm formation, both under *in vitro* and *in vivo* conditions.

Discussion

We have demonstrated for the first time that biofilm formation by *C. albicans*, the transition from yeast to hyphae morphology during biofilm formation and defects in adherence properties and biofilm formation by selective mutants can be monitored longitudinally in individual animals by using bioluminescence imaging. One of the key challenges in *Candida* biofilm research is the development of suitable *in vivo* models that account for host factors at different infection sites and that allow to evaluate the potential and efficacy of novel antifungal treatment strategies (Nett and Andes, 2006). Several *in vitro C. albicans* biofilm model systems are available to elucidate the architecture, developmental stages, cell phenotypes and drug resistance of biofilms (Nett and Andes, 2006). However, these models cannot account for the numerous host and infection-site variables that are important during infections in humans. Recently, *in vivo* central venous catheter (CVC) *C. albicans* biofilm models were

developed in rabbits, rats and mice (Andes *et al*., 2004; Schinabeck *et al*., 2004; Lazzell *et al*., 2009). Although they are extremely valuable for *C. albicans* biofilm research under *in vivo* conditions, these models have the disadvantage of being technically demanding, exposing the animals to a major surgical intervention and having a very low throughput. Řičicová *et al*. have addressed this issue and developed a rat *in vivo C. albicans* foreign body infection model in which small pieces of catheter challenged with *C. albicans* cells are subcutaneously implanted in rats (Řičicová *et al*., 2010). This model can produce similar biofilms as in the CVC models with the major advantage that up to nine catheter fragments can be implanted in one animal with only minor surgery. Although this model cannot account for factors as shear stress and nutrient flow as is observed in the blood stream, the suitability of the model to evaluate the efficacy of antifungal drugs on biofilm development was shown, allowing more rapid screening under *in vivo* conditions (Kucharíková *et al*., 2010; 2013; Bink *et al*., 2012).

Translating this rat biofilm model to mice further improved the cost-efficiency of *in vivo* screening and holds potential for biofilm research in different transgenic mouse strains that would allow for studying different host factors. Making these animal models compatible with BLI reduces the costs and number of animals needed even further. Moreover, the major advantage of BLI-compatible animal models lies in that only non-invasive imaging has the potential to provide dynamic information on the infection process and immune response in individual animals (Hutchens and Luker, 2007). In the case of bacterial pathogens, luminescent reporters based on the *lux* operon can be used, which have the advantage that there is no need for substrate addition as this is produced intracellularly (Gahan, 2012). For eukaryotic cells, other intracellularly expressed luciferases such as firefly, *Renilla* and click beetle luciferases) are available and commonly used (Badr and Tannous, 2011), but here bioluminescence relies on external substrate administration and therefore, on sufficient intracellular substrate availability. The development of BLI for imaging fungal infections has to address some additional challenges, including the fungal cell wall, which was found to be an obstacle for the intracellular substrate availability for the intracellularly located firefly luciferase (Doyle *et al*., 2006). Engineering the naturally secreted *Gaussia* luciferase to be located extracellularly partially solved the problem in the sense that superficial *C. albicans* infections could successfully be imaged with *in vivo* BLI upon topical application of its substrate CTZ (Enjalbert *et al*., 2009). However, BLI was not successful for imaging *C. albicans* infection from deeper infection sites due to yet not fully understood reasons (Enjalbert *et al*., 2009). Contributing factors might be found in some of the disadvantages that are associated with the *in vivo* use of *gLuc*; namely the emission of blue bioluminescence which is more absorbed and scattered by the tissue than light with longer wavelengths, and the rapid clearance of its substrate CTZ from the blood (Zhao *et al*., 2004; Tannous *et al*., 2005).

The challenges of BLI to visualize fungal infections were also illustrated by the work of Donat *et al*. in which a bioluminescent *Aspergillus fumigatus* strain was developed using cell wall-exposed *gLuc* (Donat *et al*., 2012). Their attempts to image pulmonary infection of this bioluminescent strain *in vivo* failed. When imaging cutaneous infection, they did observe a bioluminescent signal but could not establish a correlation between fungal load and BLI signal intensity. The latter might be explained by the high degree of instability through auto-oxidation of CTZ, which resulted in a high background signal (Shimomura *et al*., 1993; Tannous *et al*., 2005).

In our study, we also use extracellular *gLuc*, which warrants better accessibility of the substrate and is a prerequisite for a detectable bioluminescent signal *in vivo*, circumventing restricted diffusion through the fungal cell wall. Although the substrate CTZ – like any nutrient – needs to diffuse through the extracellular matrix to reach the *gLuc* expressed at the cell wall of the *Candida* cells, our results show that these challenges can be overcome and that BLI proves to be a sensitive tool providing dynamic information on biofilm development using the extracellularly located *gLuc* reporter that was originally developed by the d'Enfert-group (Enjalbert *et al*., 2009).

We have shown the feasibility of sensitive and dynamic BLI of biofilms formed on foreign bodies *in vitro*. It has the potential to be used as a rapid, easy and cost-effective screening technique for studies of *in vitro* biofilm formation, validating interesting proteins of the pathogen involved in biofilm formation as shown here for Bcr1 and assessing morphogenesis and antifungal testing. The BLI technique forms a valuable non-destructive alternative next to other alternatives for quantitative analysis of *in vitro* biofilm growth, e.g. cfu counting, XTT reduction assay, crystal violet assay or other published techniques such as the ATP bioluminescence assay (Nikawa *et al*., 1996).

More importantly, we were able to show *in vivo* BLI signal quantification from *C. albicans* biofilms developed *in vivo* on catheters implanted on the back of mice. The BLI signal intensity was in agreement with the amount of cfu recovered from explanted biofilms for validation, showing for the first time that BLI to non-invasively monitor fungal biofilm formation in live animals is feasible.

Co-registering BLI and MR images adds information on the exact position of the catheters and on tissue thickness and composition between the catheter and the BLI camera. However, prior knowledge of the exact catheter

position from MRI does not have a significant influence on the accuracy of BLI signal quantification in our model. This brings BLI as a relatively cheap tool for imaging and quantification of *in vivo* biofilm formation within the reach of many labs. When translating the technology towards other models of *in vivo* biofilm formation that involve deeper implantation sites, we anticipate that co-registration with MRI might become more important to provide information on the exact catheter position, on the nature of the surrounding tissue types or the presence of bleedings or scar formation to potentially correct for differences in light absorption and scattering properties.

When imaging *in vitro* and *in vivo* biofilms, one might expect a limited delivery of substances, for example CTZ, to the *gLuc*-expressing *C. albicans* cells inside the dense extracellular matrix in fully developed biofilms. However, studies looking at restricted penetration as a potential factor leading to increased drug resistance of biofilms have indicated that the matrix does not form a major barrier to drug diffusion (Al-Fattani and Douglas, 2004), although for some substances penetration can be delayed (Mah and O'Toole, 2001). *C. albicans* itself possesses different types of efflux pumps (Ramage *et al*., 2002), but as *gLuc* is located extracellularly, these efflux pumps are unlikely to be relevant for potentially limiting the substrate availability for the bioluminescence reactions in this study.

The observed increased background BLI signal from fully developed wt biofilms indicate that an increased amount of biomass increases the chemiluminescence of CTZ. A similar phenomenon of aspecific BLI signal from wt *C. albicans* infection sites compared with non-infected controls has been previously observed (Enjalbert *et al*., 2009), but remains unexplained. For some biomolecules like albumin and insulin it was shown that they catalyse CTZ chemiluminescence (Vassel *et al*., 2012), but for compounds that constitute biofilms, studies on their possible influence on CTZ chemiluminescence are currently lacking. Nevertheless, this observation highlights the importance of taking the necessary controls when imaging bioluminescence using CTZ.

In the case of *in vivo* BLI of biofilms in implanted catheters, the formation of fibrous scar tissue around the catheters can be an additional factor in the relatively lower specific BLI signal at later time points. This scar tissue has an influence on slowing down the diffusion of CTZ towards the catheters, which is reflected in an increased time-to-peak of the BLI signal after CTZ administration (data not shown). However, our MRI data did not indicate excessive bleeding or scar formation in individual animals.

Using a morphogenesis-dependent promoter, we showed that hyphal growth during biofilm maturation can be monitored with BLI *in vitro* and in live animals. The change in specific BLI signal from hyphal cells was most pronounced during the first stages of mature biofilm formation, as most cells go through the transition from the yeast to the hyphal cell stage (Blankenship and Mitchell, 2006). Once a mature biofilm is formed, the differences between the specific hyphal BLI signal and the BLI signal driven by the *ACT1* promoter are less pronounced. This might reflect the hyphal content of the biofilm at this stage (Nett and Andes, 2006). In this context, it is of note that the activity of the *ACT1* promoter is not constant throughout the different stages of biofilm formation (Nailis *et al*., 2006). It would be of interest to add BLI studies on morphogenesis of biofilms using a yeast cell stage specific promoter for *gLuc* expression and/or mutants defective in hyphae formation i.e. that do not express the hyphal cell wall protein (Baillie and Douglas, 1999).

We also demonstrated that BLI can be used to monitor the role of a gene involved in biofilm formation. By engineering the *bcr1*$^{-/-}$ mutant *C. albicans* to be bioluminescent, we could visualize and quantify its hampered substrate adherence and inability to form normal biofilms *in vitro* and *in vivo*, which is a known effect of the double *BCR1* knockout in this strain (Nobile *et al*., 2006; Řičicová *et al*., 2010). BLI shows to be a powerful tool to dynamically monitor the function of genes involved in biofilm formation, thereby opening the door towards more rapid and convenient screening and validation of genes of the pathogen playing a role in biofilm formation and dynamic follow-up of the interplay between pathogen and substrate within the living host.

Conclusion & perspectives

We have demonstrated the feasibility of using BLI to non-invasively and longitudinally monitor biofilm development and morphogenesis in subcutaneously implanted catheters in rodents. We expect this approach to be readily translatable to other biofilm models such as the CVC model as the intravenous (iv) catheter is located not too deep under the skin and iv CTZ injection might result in a favourable substrate delivery and reproducibility of BLI results. Studies are underway to evaluate the feasibility of BLI for *in vivo* biofilm research in the CVC model that will enable to account for factors as shear stress and nutrient flow on biofilm formation. The here described multi-temporal non-invasive imaging tool for quantifying *in vitro* and *in vivo* biofilm formation has the potential for applications in the screening and validation of antifungal drugs under *in vivo* conditions, for studying host–biofilm interactions in different transgenic mouse models and for studying the virulence of mutant *C. albicans* in this luminescent background, and hereby contribute to a better understanding of the pathogenesis of yeast infections during biofilm formation.

Experimental procedures

Strains and culture media

Wild-type *C. albicans* SC5314, a clinical isolate with a successfully sequenced genome (Gillum *et al*., 1984) was used as a control strain in these studies. This strain was engineered to express *C. albicans* codon-optimized *Gaussia princeps* luciferase (*gLuc*) at the cell wall, under the control of a constitutive (actin, *ACT1*) and a hyphal growth phase-specific (*HWP1*) promoter. SC5314 was transformed in the RPS1 locus with the Clp10::Act1p-gLUC59 plasmid (Enjalbert *et al*., 2009), kindly provided to us by Prof. C. d'Enfert, in which we replaced the *URA3* transformation marker with *SAT1*. Positive transformants were identified by BLI and confirmed by PCR. Two bioluminescent transformants (SKCA23-*ACTgLuc* and SKCA43-*ACTgLuc*) that were normal regarding hyphal induction and growth (data not shown) were selected for both *in vitro* and *in vivo* biofilm bioluminescence assays. These strains express *gLuc* fused to the endogenous *PGA59* gene under the control of the *ACT1* promoter. The results with both strains were similar and all data presented in this paper were obtained with SKCA23-*ACTgLuc*.

Similarly, we transformed the mutant *C. albicans* CJN702 - *bcr1/bcr1* (*ura3Δ*::λ*imm434/ura3Δ*::λ*imm434 arg4::hisG/arg4::hisG his1*::*hisG/his1*::*hisG*::*pHIS1 bcr1*::*ARG4/bcr1*::*URA3*) (Nobile and Mitchell, 2005) with the Clp10::Act1p-gLUC59 plasmid, resulting in the bioluminescent strain further referred to as *bcr1*$^{-/-}$*-ACTgLuc*.

Also used in this study were strains CEC971 (*HWP1p-PGA59-gLUC*, morphogenesis-dependent expressing of *gLuc*, further referred to as CEC971-*HWPgLuc*), CEC988 (*ACT1p-PGA59-gLUC*, further referred to as CEC988-*ACTgLuc*) and DAY185 (wt control), kindly provided to us by Prof. C. d'Enfert (Enjalbert *et al*., 2009).

In vitro *biofilm formation*

Strains were grown overnight on YPD plates at 37°C, washed and resuspended in PBS. The cells were counted to prepare a *C. albicans* cell suspension in RPMI medium (RPMI-1640, R6504, Sigma-Aldrich, Diegem, Belgium; with L-glutamine and without sodium carbonate buffered with MOPS, pH 7.0). To study biofilm formation *in vitro*, sterile 96-well (24-well) polystyrene cell culture plates were inoculated by adding 100 µl (200 µl) per well of a 1×10^7 cells ml^{-1} *C. albicans* cell suspension in RPMI. The *C. albicans* cells were allowed to adhere to the bottom of the wells by incubating the plate for 90 min at 37°C. After washing twice with PBS, attached cells were submerged in 200 µl (96-well plate) or 1 ml (24-well plate) of fresh RPMI medium and the plate was again incubated at 37°C for the duration of the experiment to allow formation of mature biofilms. To study biofilm formation on the inside of a catheter *in vitro*, polyurethane triple-lumen intravenous catheters (2.4 mm diameter, Certofix Trio S730, BBraun, Diegem, Belgium) were cut into 1 cm long fragments and incubated overnight with FBS (F7524, Sigma) at 37°C. A *C. albicans* cell suspension of 5×10^4 cells ml^{-1} was added to the catheters placed in a 24-well plate and incubated for 90 min at 37°C for adhesion. Catheters were washed twice with PBS, transferred to a clean plate and submerged in 1 ml of fresh RPMI medium and incubated at 37°C for the duration of the experiment.

In vitro *BLI*

To obtain *in vitro* bioluminescence measurements, the plates containing cell suspensions, biofilms formed on the bottom of cell culture plates or biofilms formed inside catheter pieces were placed in a BLI-camera (IVIS 100, Perkin-Elmer, Waltham, MA, USA). For all *in vitro* experiments, a native coelenterazine (CTZ; Nanolight Technologies, Pinetop, AZ, USA) working solution in PBS was prepared freshly from a 5 mg ml^{-1} stock solution in acidified ethanol, prepared and stored at −80°C according to the manufacturer's instructions. After acquisition of a background image, CTZ was added to the wells at a final concentration of 6 µM. Subsequent frames were acquired with a 5–20 s exposure time depending on the signal intensity, at medium binning. The BLI signal was quantified using Living Image software (version 2.50.1, provided by the manufacturer) and reported as photon flux per second (p s^{-1}) for a given ROI of fixed size covering the well or catheter (for more details, see Vande Velde *et al*., 2013). *In vitro* BLI data were normalized to the background signal from CTZ alone unless stated otherwise.

Animals

Female, 8-week-old Balb/C mice and Sprague-Dawley rats of 200 g (Janvier, Le Genest Saint-Isle, France) were used for *in vivo* biofilm studies. The animals were kept in individually ventilated filter top cages with free access to standard food and water *ad libitum*. All animals were immunosuppressed starting 24 h before and during the entire experiment by adding dexamethasone (0.4 mg l^{-1}; Fagron SAS, Paris, France) to their drinking water. Ampicillin (ampicillin sodium powder 0.5 g l^{-1}; Duchefa Biochemie, Haarlem, the Netherlands) was also added to the water to prevent possible bacterial infections. All aspects of animal experiments were carried out in compliance with national and European regulations and were approved by the animal ethics committee of the KU Leuven.

In vivo *biofilm model*

Catheter segments of 1 cm length were incubated overnight in FBS (100%) at 37°C. Serum-coated catheters were incubated for 90 min at 37°C in a 1 ml *C. albicans* cell suspension (5×10^4 cells ml^{-1} prepared in RPMI). After incubation, catheters were washed twice with PBS before implanting them under the skin of mice or rats as described previously, with minor adaptations (Řičicová *et al*., 2010). In brief, general anesthesia was performed by intraperitoneal injection of a mixture of ketamine (Ketamine1000®; Pfizer, Puurs, Belgium) and medetomidine (Domitor®; Pfizer) (45 mg kg^{-1} ketamine and 0.6 mg kg^{-1} medetomidine for mice, 60 mg kg^{-1} ketamine and 0.4 mg kg^{-1} medetomidine for rat) and local anaesthesia by application of xylocaine gel (2%, AstraZeneca, Zoetermeer, the Netherlands) on the skin. The lower back of the animals was shaved and disinfected with iodine isopropanol (1%). A small incision was made and the subcutis was carefully dissected to create two (for mice) or three (for rats) subcutaneous tunnels. In each tunnel, three catheter pieces were inserted. In total, six (for mice) or nine (for rats) catheter fragments were implanted (see Vande Velde *et al*., 2013 for more details). The incision was closed with surgical staples or sutured with surgical thread and disinfected.

Anesthesia was reversed with intraperitoneal injection of atipamezole [Antisedan® (Pfizer), 0.5 mg kg^{-1} for mice, 1 mg kg^{-1} for rats]. For catheter explantation, the animals were euthanized by cervical dislocation. The skin was disinfected with 0.5% chlorhexidine in 70% alcohol; catheter fragments were removed from under the subcutaneous tissue and washed twice with PBS for further quantification of biomass.

Magnetic resonance imaging (MRI)

MR images were acquired on a 9.4 Tesla Biospec small animal scanner (Bruker Biospin, Ettlingen, Germany) equipped with an actively shielded gradient set of 600 mT m^{-1} and in combination with a 7.5 cm quadrature coil (Bruker Biospin) for radio-frequency irradiation and detection. The mice were anesthetized by inhalation of 3% isoflurane (Abbott Laboratories, Queenborough, UK) for induction and 1.5% isoflurane for maintenance in 100% O_2 at a flow rate of 600 ml min^{-1}. Breathing rate and body temperature were continuously monitored using an MR compatible physiological monitoring system (SAII, Stony Brook, NY, USA). Localizer images were acquired first and used for proper positioning and orientation of subsequently acquired images. Whole-body images were acquired with an in-plane resolution of 200*200 μm^2 using a 2D spin echo sequence (RARE) with the following parameters: RARE factor = 8, TE_{eff} = 15.9 ms, TR = 6000 ms, 2 averages, matrix = 200*400, FOV = 40*80 mm^2, 50 continuous slices of 500 μm thickness; resulting in a total scanning time of ~ 12 min. MR images were processed using Paravision 5.1 software (Bruker Biospin) and exported in Dicom format. For co-registration of BLI and MR images, the photographic image from BLI was overlaid with the whole-body MR image using in-house developed software (Carlon *et al.*, 2010). Hereby, limb position and size were used as reference points.

In vivo *BLI*

The animals were anesthetized using a gas mixture of isoflurane in oxygen (1.5–2% for mice and 2–3% for rats) and imaged in the IVIS 100 system. Before every *in vivo* imaging session, the 1.2 mM CTZ working solution was prepared freshly from a 5 mg ml^{-1} stock solution by dilution in PBS. A volume of 100 μl CTZ was topically applied simultaneously to each catheter trio by subcutaneous injection in each tunnel. Subsequently, the animal was placed in the BLI camera and consecutive frames were acquired with a field of view of 10 cm. Consecutive scans with acquisition time of 20–60 s (depending on the signal intensity) were acquired starting immediately (i.e. within 10 s) after CTZ administration until maximum signal intensity was reached. The BLI signal of each catheter trio was quantified using Living Image software and reported as photon flux per second (p s^{-1}) for a rectangular ROI of 95 cm^2 placed over each catheter trio. Background BLI signal was measured by using the same ROI after injecting CTZ subcutaneously on the upper back of the mouse (no catheters implanted). All *in vivo* experiments were repeated twice with similar results.

Biofilm quantification

The metabolic activity of the biofilm forming cells was quantified by using the XTT reduction assay, Biofilms formed on 96-well plates were washed twice with PBS and 100 μl of XTT-solution (1 mg ml^{-1}) supplemented with menadion (1 μM) was added in the absence of light. Plates were subsequently incubated at 37°C for 1–3 h and the colorimetric changes were measured with a spectrophotometer (SPECTRAmax plus 384, Molecular Devices, Sunnyvale, CA, USA) at 490 nm.

For fungal burden assessment by cfu quantification, biofilms formed on cell culture plates, in *in vitro* evaluated catheters and explanted catheters were washed twice with PBS, sonicated for 10 min at 40 000 Hz in a water bath sonicator (Branson 2210) and vortexed for 30 s in PBS. Original samples, 1:10 and 1:100 dilutions were plated on YPD agar in duplicate. Cfu were counted after incubating the plates for 2 days at 37°C.

Statistics

All reported experiments were repeated twice and analysed separately, yielding consistent results. Data were expressed as mean ± standard deviation (SD). Significance tests were performed using unpaired *t*-test and ANOVA with Tukey post-test with *P*-values of < 0.05 considered significant, represented as follows: $*P < 0.05$, $**P < 0.005$, $***P < 0.0005$. For statistics and representation of the results we used Microsoft Office Excel 2007 (Microsoft Corporation, Seattle, WA, USA) and GraphPad Prism 5 (GraphPad Software, La Jolla, CA, USA).

Acknowledgements

This work was funded by KU Leuven PF 'IMIR', the Fund for Scientific Research Flanders (FWO: WO.026.11N and G.0804.11), and by the Interuniversity attraction poles programme initiated by the Belgian Science Policy office. SK gratefully acknowledges grants from the KU Leuven (PDMK 11/089) and the FWO.

We thank Prof. Christophe d'Enfert for providing us with the Clp10::ACT1p-gLUC59 plasmid and *C. albicans* CEC971 and CEC988 strains and Prof. A. Mitchell for *C. albicans* DAY185 and CJN702-*bcr1/bcr1* knockout strains. We are grateful to Deborah Seys and Ilse Palmans for their excellent technical assistance.

Conflict of interest

The authors declare no conflict of interest.

References

Al-Fattani, M.A., and Douglas, L.J. (2004) Penetration of *Candida* biofilms by antifungal agents. *Antimicrob Agents Chemother* **48:** 3291–3297.

Andes, D., Nett, J., Oschel, P., Albrecht, R., Marchillo, K., and Pitula, A. (2004) Development and characterization of an in vivo central venous catheter *Candida albicans* biofilm model. *Infect Immun* **72:** 6023–6031.

Badr, C.E., and Tannous, B.A. (2011) Bioluminescence imaging: progress and applications. *Trends Biotechnol* **29:** 624–633.

Baillie, G.S., and Douglas, L.J. (1999) Role of dimorphism in the development of *Candida albicans* biofilms. *J Med Microbiol* **48:** 671–679.

Bink, A., Kucharíková, S., Neirinck, B., Vleugels, J., Van Dijck, P., Cammue, B.P., and Thevissen, K. (2012) The nonsteroidal antiinflammatory drug diclofenac potentiates the in vivo activity of caspofungin against *Candida albicans* biofilms. *J Infect Dis* **206:** 1790–1797.

Biswas, S., Van Dijck, P., and Datta, A. (2007) Environmental sensing and signal transduction pathways regulating morphopathogenic determinants of *Candida albicans*. *Microbiol Mol Biol Rev* **71:** 348–376.

Blankenship, J.R., and Mitchell, A.P. (2006) How to build a biofilm: a fungal perspective. *Curr Opin Microbiol* **9:** 588–594.

Brock, M. (2012) Application of bioluminescence imaging for in vivo monitoring of fungal infections. *Int J Microbiol* **2012:** 956794.

Carlon, M., Toelen, J., Van der Perren, A., Vandenberghe, L.H., Reumers, V., Sbragia, L., *et al*. (2010) Efficient gene transfer into the mouse lung by fetal intratracheal injection of rAAV2/6.2. *Mol Ther* **18:** 2130–2138.

Chen, S.C., Playford, E.G., and Sorrell, T.C. (2010) Antifungal therapy in invasive fungal infections. *Curr Opin Pharmacol* **10:** 522–530.

Contag, C.H., Contag, P.R., Mullins, J.I., Spilman, S.D., Stevenson, D.K., and Benaron, D.A. (1995) Photonic detection of bacterial pathogens in living hosts. *Mol Microbiol* **18:** 593–603.

d'Enfert, C., Vecchiarelli, A., and Brown, A.J.P. (2010) Bioluminescent fungi for real-time monitoring of fungal infections. *Virulence* **1:** 174–176.

Donat, S., Hasenberg, M., Schafer, T., Ohlsen, K., Gunzer, M., Einsele, H., *et al*. (2012) Surface display of *Gaussia* princeps luciferase allows sensitive fungal pathogen detection during cutaneous aspergillosis. *Virulence* **3:** 51–61.

Douglas, L.J. (2003) *Candida* biofilms and their role in infection. *Trends Microbiol* **11:** 30–36.

Doyle, T.C., Nawotka, K.A., Kawahara, C.B., Francis, K.P., and Contag, P.R. (2006) Visualizing fungal infections in living mice using bioluminescent pathogenic *Candida albicans* strains transformed with the firefly luciferase gene. *Microb Pathog* **40:** 82–90.

Eggimann, P., Garbino, J., and Pittet, D. (2003a) Epidemiology of *Candida* species infections in critically ill non-immunosuppressed patients. *Lancet Infect Dis* **3:** 685–702.

Eggimann, P., Garbino, J., and Pittet, D. (2003b) Management of *Candida* species infections in critically ill patients. *Lancet Infect Dis* **3:** 772–785.

Enjalbert, B., Rachini, A., Vediyappan, G., Pietrella, D., Spaccapelo, R., Vecchiarelli, A., *et al*. (2009) A multifunctional, synthetic *Gaussia princeps* luciferase reporter for live imaging of *Candida albicans* infections. *Infect Immun* **77:** 4847–4858.

Enoch, D.A., Ludlam, H.A., and Brown, N.M. (2006) Invasive fungal infections: a review of epidemiology and management options. *J Med Microbiol* **55:** 809–818.

Fisher, M.C., Henk, D.A., Briggs, C.J., Brownstein, J.S., Madoff, L.C., McCraw, S.L., and Gurr, S.J. (2012) Emerging fungal threats to animal, plant and ecosystem health. *Nature* **484:** 186–194.

Gahan, C.G. (2012) The bacterial *lux* reporter system: applications in bacterial localisation studies. *Curr Gene Ther* **12:** 12–19.

Gillum, A.M., Tsay, E.Y., and Kirsch, D.R. (1984) Isolation of the *Candida albicans* gene for orotidine-5′-phosphate decarboxylase by complementation of *S. cerevisiae ura3* and *E. coli pyrF* mutations. *Mol Gen Genet* **198:** 179–182.

Giri, S., and Kindo, A.J. (2012) A review of *Candida* species causing blood stream infection. *Indian J Med Microbiol* **30:** 270–278.

Hawser, S.P., and Douglas, L.J. (1995) Resistance of *Candida albicans* biofilms to antifungal agents in vitro. *Antimicrob Agents Chemother* **39:** 2128–2131.

Hutchens, M., and Luker, G.D. (2007) Applications of bioluminescence imaging to the study of infectious diseases. *Cell Microbiol* **9:** 2315–2322.

Kim, J., and Sudbery, P. (2011) *Candida albicans*, a major human fungal pathogen. *J Microbiol* **49:** 171–177.

Kucharíková, S., Tournu, H., Lagrou, K., Van Dijck, P., and Bujdakova, H. (2011) Detailed comparison of *Candida albicans* and *Candida glabrata* biofilms under different conditions and their susceptibility to caspofungin and anidulafungin. *J Med Microbiol* **60:** 1261–1269.

Kucharíková, S., Tournu, H., Holtappels, M., Van Dijck, P., and Lagrou, K. (2010) In vivo efficacy of anidulafungin against mature *Candida albicans* biofilms in a novel rat model of catheter-associated Candidiasis. *Antimicrob Agents Chemother* **54:** 4474–4475.

Kucharíková, S., Sharma, N., Spriet, I., Maertens, J., Van Dijck, P., and Lagrou, K. (2013) Activity of systemically administered echinocandins against in vivo mature *Candida albicans* biofilms developed in a rat subcutaneous model. *Antimicrob Agents Chemother* **57:** 2365–2368.

Lazzell, A.L., Chaturvedi, A.K., Pierce, C.G., Prasad, D., Uppuluri, P., and Lopez-Ribot, J.L. (2009) Treatment and prevention of *Candida albicans* biofilms with caspofungin in a novel central venous catheter murine model of candidiasis. *J Antimicrob Chemother* **64:** 567–570.

Lewis, R.E., Kontoyiannis, D.P., Darouiche, R.O., Raad, I.I., and Prince, R.A. (2002) Antifungal activity of amphotericin B, fluconazole, and voriconazole in an in vitro model of *Candida* catheter-related bloodstream infection. *Antimicrob Agents Chemother* **46:** 3499–3505.

Mah, T.F., and O'Toole, G.A. (2001) Mechanisms of biofilm resistance to antimicrobial agents. *Trends Microbiol* **9:** 34–39.

Nailis, H., Coenye, T., Van Nieuwerburgh, F., Deforce, D., and Nelis, H.J. (2006) Development and evaluation of different normalization strategies for gene expression studies in *Candida albicans* biofilms by real-time PCR. *BMC Mol Biol* **7:** 25.

Nett, J., and Andes, D. (2006) *Candida albicans* biofilm development, modeling a host-pathogen interaction. *Curr Opin Microbiol* **9:** 340–345.

Nikawa, H., Nishimura, H., Yamamoto, T., Hamada, T., and Samaranayake, L.P. (1996) The role of saliva and serum in *Candida albicans* biofllm formation on denture acrylic surfaces. *Microbial Ecology in Health and Disease* **9:** 35–48.

Nobile, C.J., and Mitchell, A.P. (2005) Regulation of cell-surface genes and biofilm formation by the *C. albicans* transcription factor Bcr1p. *Curr Biol* **15:** 1150–1155.

Nobile, C.J., Andes, D.R., Nett, J.E., Smith, F.J., Jr, Yue, F., Phan, Q.-T., *et al*. (2006) Critical role of Bcr1-dependent

adhesins in *C. albicans* biofilm formation in vitro and in vivo. *PLoS Pathog* **2:** e63.
Nucci, M., and Marr, K.A. (2005) Emerging fungal diseases. *Clin Infect Dis* **41:** 521–526.
Pemán, J., and Salavert, M. (2012) Epidemiología general de la enfermedad fúngica invasora. *Enferm Infecc Microbiol Clin* **30:** 90–98.
Pfaller, M.A., and Diekema, D.J. (2010) Epidemiology of invasive mycoses in North America. *Crit Rev Microbiol* **36:** 1–53.
Ramage, G., Bachmann, S., Patterson, T.F., Wickes, B.L., and Lopez-Ribot, J.L. (2002) Investigation of multidrug efflux pumps in relation to fluconazole resistance in *Candida albicans* biofilms. *J Antimicrob Chemother* **49:** 973–980.
Řičicová, M., Kucharíková, S., Tournu, H., Hendrix, J., Bujdakova, H., Van Eldere, J., *et al*. (2010) *Candida albicans* biofilm formaton in a new in vivo rat model. *Microbiology* **156:** 909–919.
Schinabeck, M.K., Long, L.A., Hossain, M.A., Chandra, J., Mukherjee, P.K., Mohamed, S., and Ghannoum, M.A. (2004) Rabbit model of *Candida albicans* biofilm infection: liposomal amphotericin B antifungal lock therapy. *Antimicrob Agents Chemother* **48:** 1727–1732.
Shimomura, O., Kishi, Y., and Inouye, S. (1993) The relative rate of aequorin regeneration from apoaequorin and coelenterazine analogues. *Biochem J* **296** (Part 3)**:** 549–551.
Sjolinder, H., and Jonsson, A.B. (2007) Imaging of disease dynamics during meningococcal sepsis. *PLoS ONE* **2:** e241.
Staab, J.F., Ferrer, C.A., and Sundstrom, P. (1996) Developmental expression of a tandemly repeated, proline-and glutamine-rich amino acid motif on hyphal surfaces on *Candida albicans*. *J Biol Chem* **271:** 6298–6305.
Sudbery, P.E. (2011) Growth of *Candida albicans* hyphae. *Nat Rev Microbiol* **9:** 737–748.
Tannous, B.A., Kim, D.E., Fernandez, J.L., Weissleder, R., and Breakefield, X.O. (2005) Codon-optimized *Gaussia* luciferase cDNA for mammalian gene expression in culture and in vivo. *Mol Ther* **11:** 435–443.
Vande Velde, G., Kucharikova, S., Dijck, P.V., and Himmelreich, U. (2013) Bioluminescence imaging of fungal biofilm development in live animals. *Methods Mol Biol* **1098,** chapter 13. (in press)
Vassel, N., Cox, C.D., Naseem, R., Morse, V., Evans, R.T., Power, R.L., *et al*. (2012) Enzymatic activity of albumin shown by coelenterazine chemiluminescence. *Luminescence* **27:** 234–241.
Warnock, D.W. (2006) Fungal diseases: an evolving public health challenge. *Med Mycol* **44:** 697–705.
Wisplinghoff, H., Bischoff, T., Tallent, S.M., Seifert, H., Wenzel, R.P., and Edmond, M.B. (2004) Nosocomial bloodstream infections in US hospitals: analysis of 24,179 cases from a prospective nationwide surveillance study. *Clin Infect Dis* **39:** 309–317.
Zhao, H., Doyle, T.C., Wong, R.J., Cao, Y., Stevenson, D.K., Piwnica-Worms, D., and Contag, C.H. (2004) Characterization of coelenterazine analogs for measurements of Renilla luciferase activity in live cells and living animals. *Mol Imaging* **3:** 43–54.

Supporting information

Additional Supporting Information may be found in the online version of this article at the publisher's web-site:

Fig. S1. Phosphorescence of different common catheter types. Three different brands of triple lumen catheters (Arrow, Edwards Swan-Ganz, BBraun Certofix) were cut in 1 cm long pieces and placed in Petri dishes for image acquisition with the BLI camera. Panel A: luminescence image acquired after exposing the catheters to light by opening-closing of the scanner door, showing phosphorescence signal emitted by the triple-lumen Swan-Ganz and Arrow catheter pieces, while no phosphorescence signal was detected for the Certofix catheter pieces. Panel B is the same image as in panel A, showing the overlaid ROIs used for quantification of the background and phosphorescence signals as plotted in Fig. 1A.
Fig. S2. BLI of yeast-to-hyphal cell ratio. *HWPgLuc*-expressing *C. albicans* cells were cultured either to be in the yeast cell from (in YPD medium) or in the hyphal cell form (YP medium containing 10% fetal bovine serum). *Candida* yeast and/or hyphal cell suspensions of 1×10^7 cells ml^{-1} were plated in 24-well plates, in a total volume of 1 ml medium, imaged with BLI in triplicate series as follows: *HWPgLuc*-expressing *C. albicans* hyphal/yeast cells in ratios (%): 100/0–80/20–60/40–40–60–20/80–0/100. The graph represents the BLI results and linear regression line ($R^2 = 0.9559$), showing near-perfect correlation of the bioluminescence signal intensity with the percentage hyphal content in the sample. Error bars are StDev of triplicate samples.
Fig. S3. BLI of planktonic *bcr1*$^{-/-}$*-ACTgLuc* cells.
A. BLI of 10-fold dilutions of *bcr1*$^{-/-}$*-ACTgLuc* and SC5314-*ACTgLuc* (wt control) *C. albicans* cells, and CTZ alone ($n = 3$). The BLI-signal emitted from *bcr1*$^{-/-}$*-ACTgLuc* and SC5314-*ACTgLuc C. albicans* was found to be equal and correlated strongly with the number of cells. (R^2 (*bcr1*$^{-/-}$*-ACTgLuc*) = 0.957, R^2 (SC5314-*ACTgLuc*) = 0.999).
B. BLI signal (left graph) and cfu (right graph) quantified from the planktonic cells collected from the lumen of explanted catheters at different time points of biofilm formation by *bcr1*$^{-/-}$*-ACTgLuc* and SC-*ACTgLuc C. albicans* strains. The means of triplicate samples per catheter ($n = 18$) were plot. Error bars indicate SD of replicate samples; $^*P < 0.05$, $^{**}P < 0.005$, $^{***}P < 0.0005$).